Soft Matter

Accepted Manuscript

ROYAL SOCIETY OF CHEMISTRY

www.rsc.org/softmatter

Weaving colloidal webs around droplets – Spontaneous assembly of extended colloidal networks encasing microfluidic droplet ensembles

Lu Zheng[♀], *Leon Yoon Ho*[♀] and *Saif A. Khan*[♀*]

[♀]Department of Chemical and Biomolecular Engineering, 4 Engineering Drive 4, National University of Singapore, Singapore 117585, Singapore

[*]Corresponding Author. Email: saifkhan@nus.edu.sg

KEYWORDS: Diffusive Self-assembly, Host-guest Inclusion complexes, Droplet microfluidics, Materials Synthesis, Spherical Crystallization

GRAPHICAL ABSTRACT

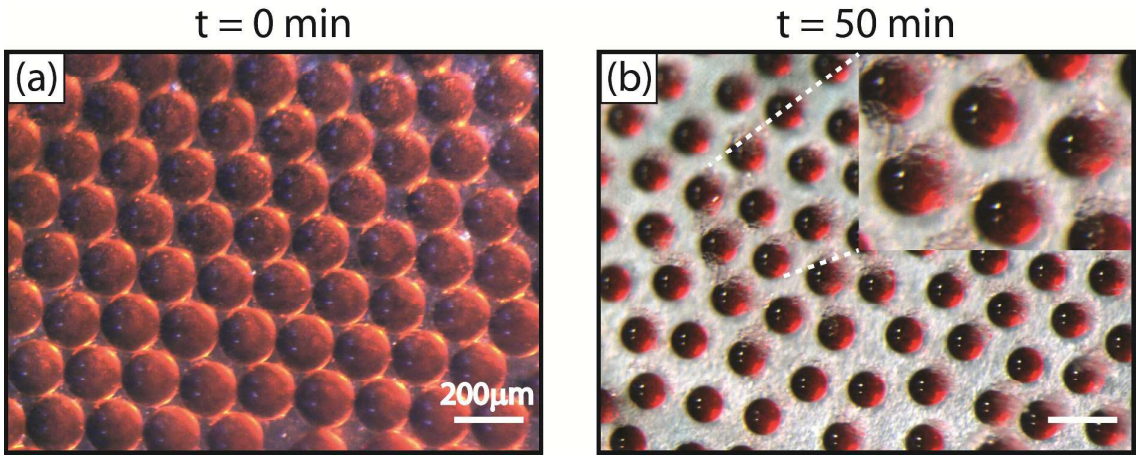

We demonstrate transient, self-assembling solid networks that 'cocoon' emulsion droplets on-demand, and allow new possibilities in microfluidic droplet-based materials science.

Weaving colloidal webs around droplets – Spontaneous assembly of extended colloidal networks encasing microfluidic droplet ensembles

Lu Zheng[♀], *Leon Yoon Ho*[♀] and *Saif A. Khan*[♀*]

[♀]Department of Chemical and Biomolecular Engineering, 4 Engineering Drive 4, National University of Singapore, Singapore 117585, Singapore

[*]Corresponding Author. Email: saifkhan@nus.edu.sg

KEYWORDS: Diffusive Self-assembly, Host-guest Inclusion complexes, Droplet microfluidics, Materials Synthesis, Spherical Crystallization

ABSTRACT

The ability to form transient, self-assembling solid networks that 'cocoon' emulsion droplets on-demand allows new possibilities in the rapidly expanding area of microfluidic droplet-based materials science. In this paper, we demonstrate the spontaneous formation of extended colloidal networks that encase large microfluidic droplet ensembles, thus completely arresting droplet motion and effectively isolating each droplet from others in the ensemble. To do this, we employ molecular inclusion complexes of β-cyclodextrin, which spontaneously form and assemble into colloidal solids at the droplet interface and beyond, via the outward diffusion of a guest molecule (dichloromethane) from the droplets. We illustrate the advantage of such transient network-based droplet stabilization in the area of pharmaceutical crystallization, where we are able to fabricate monodisperse spherical crystalline microgranules of 5-methyl-2-[(2-nitrophenyl)amino]-3-thiophenecarbonitrile (ROY), a model hydrophobic drug, with dramatic enhancement of particle properties compared to conventional methods.

Droplet-based microfluidics, which allows the creation of exquisitely controlled emulsions, has led to rapid advances in the science and controlled manufacture of advanced microscale materials on the one hand, and in high throughput chemical or biological screening on the other.[1,2] Therefore, there has been a lot of interest in both the generation of droplets, and also in their stabilization via appropriate choice of fluids and surfactants.[3-5] The latter issue is as critical as the former, since a large fraction of applications involves the creation of droplets with specific chemical/biological contents, followed by incubation for extended periods of time, either in flowing or static fashion; therefore, the nominal isolation of droplets and prevention of interface breakage/coalescence become paramount requirements. In this context, there is considerable interest in *particle*-stabilized emulsions,[6-11] where interfacial stability is conferred by irreversible adsorption of (colloidal) particles at the interface.[8,12] Rather than lowering the interfacial tension as surfactants do, the permanent physical barriers prevent coalescence, thus granting particle-stabilized systems remarkable stability compared to surfactant stabilized systems.[9] *Network* stabilization using crystals is another related scheme for emulsion stabilization, and is widely applied in food industry (in table spreads, baking, etc.). In this scheme, fat-based crystal networks in the continuous phase are used to reduce flocculation and coalescence by physically separating the droplets from one another.[13-16]

In this paper, we combine the schemes of particle *and* network stabilization, and demonstrate the spontaneous formation of extended colloidal networks that encase large microfluidic droplet ensembles, thus completely arresting droplet motion and effectively isolating each droplet from others in the ensemble. To do this, we employ molecular inclusion complexes (ICs), formed at the water-oil interface from cyclodextrins and a wide range of guest molecules, such as lipids (fatty acids, glycerides) or long chain alkanes. ICs are a particularly interesting class of materials that have been recently demonstrated to form particle-stabilized emulsion systems.[10,11,17-20] The ICs form instantaneously at the oil-water

interface via non-covalent interactions between the cyclodextrin (host) cavity and the guest molecule, and subsequently assemble into colloidal solids that stabilize the interface.[10,21] In our method, a *volatile* guest molecule (dichloromethane) diffuses radially outward from an ensemble of static, dispersed droplets, to spontaneously form ICs with aqueous β-cyclodextrin in the continuous phase, which assemble into colloidal solids at the oil-water interface and beyond, forming an extended crystal network. We further show how the resultant network is transient, with a lifetime that depends on the rate at which the volatile guest molecule leaves the system. Finally, we illustrate the advantage of such transient network-based stabilization in the area of pharmaceutical crystallization, where we are able to fabricate monodisperse crystalline microgranules of 5-methyl-2-[(2-nitrophenyl)amino]-3-thiophenecarbonitrile (ROY), a model hydrophobic drug, with dramatic enhancement of particle properties compared to conventional methods. The ability to form transient, self-assembling solid networks that 'cocoon' emulsion droplets *on-demand* expands the possibilities in (micro)droplet-based materials and analytical science.

RESULTS AND DISCUSSION

In our method, dichloromethane (DCM) is used to form oil-in-water (O/W) emulsions in an aqueous solution of polyvinyl alcohol (PVA), the latter acting as the continuous phase, in a micro-capillary emulsion generator[22,23] (see Experimental Section for details). A fixed quantity of emulsion is collected into a glass petri dish containing a pre-dispensed film of aqueous β-cyclodextrin solution, and allowed to settle into a static, single-layered ensemble of closely-packed droplets, as shown in the schematic of Figure 1. DCM-β-cyclodextrin ICs form instantaneously at the emulsion interface, and assemble into crystalline colloidal particles.[24] As DCM further diffuses from droplets into the continuous phase under a concentration gradient, it forms and precipitates more colloidal particles, eventually forming a three-dimensional colloidal crystalline network, which isolates the droplets completely from one another,

while also immobilizing the ensemble. Since the system is open, the volatile DCM eventually leaves the crystal network, leading to de-complexation of the ICs, and dissolution of the crystalline network.

In a typical experiment, approximately 50 μL of O/W emulsions generated from the capillary microfluidic device were dispensed directly into a glass petri dish containing a 2 mm thick film of 1 wt% β-cyclodextrin aqueous solution, which was placed directly on a hot plate. The aqueous continuous phase within the microfluidic device did not contain any β-cyclodextrin, since the transit time of the generated droplets in the microfluidic device (~20 s) was too short to form any observable networks. The high monodispersity of the droplets led to their rapid assembly into a hexagonally close-packed network within the aqueous film (see Figure 1b). Solvent (DCM) evaporated from the droplets (starting diameter of ~160 μm) at a measured hot plate temperature of ~25 ^{o}C, and at ambient humidity (~55%). The use of a hot plate, even at nominally ambient temperature, was necessitated by the high volatility of DCM (boiling point ~40 ºC) and thus the high sensitivity of DCM transport (diffusion and evaporation) to temperature. As shown in Figure 1a, there was an almost instantaneous onset of turbidity as the DCM droplets made contact with β-cyclodextrin aqueous solution, indicating the formation of colloids in the aqueous solution. β-cyclodextrin has been reported to form insoluble inclusion complexes instantaneously with a variety of oils and some organic solvents,[10,11,17,24-26] including DCM, as reported by Lantz *et. al*.[24] We further validated this inference with a simple, physically analogous experiment comprising a planar O/W interface within a glass vial to harvest crystalline ICs for further characterization (see Experimental Section). SEM observations of the harvested solids (Figure 1c inset) confirmed that the IC aggregates were crystalline particles in the colloidal (sub-micron) size range. Further, and crucially, as shown in Figure 1(a)-(c), with time we observed the formation of a continuous turbid *network* around the closely packed and static ensemble of droplets, which completely precluded relative droplet motion, contact and coalescence. Given the rapid observed rate of IC formation and aggregation, the dynamics of network formation was controlled by the diffusion of DCM away from the

droplets and into the continuous aqueous phase. As DCM diffused away from the droplet surface through the β-cyclodextrin aqueous solution, ICs were continuously formed and precipitated along the diffusion pathway of DCM, forming a three-dimensional network of colloidal crystalline particles encasing each droplet, which completely isolated the droplets from each other. Crucially, this turbid network formed from aggregated IC crystals was *transient*; depletion of the DCM droplets and evaporation of the dissolved DCM from the aqueous solution led to its gradual disappearance with time (Figure 1(d)). Depletion of DCM led to de-complexation of the bound DCM from the solid network, leaving behind water-soluble colloidal β-cyclodextrin crystals, which then dissolved back to the β-cyclodextrin aqueous phase.

A simple model for diffusion from a hexagonally patterned planar array of point sources releasing material at a time-dependent rate sheds further light on the dynamics of network formation.[27] In this model, each droplet is treated as a point source that continuously releases DCM, at a pre-defined, time-dependent rate (for details of the model setup and parameters used, please see the Supporting Information). The DCM subsequently diffuses away into the surrounding medium (water). We generate time-dependent 2-D plots (Figure 2) of DCM concentration in the medium; these plots enable us to make two key observations. Firstly, if we assume that there exists some critical concentration of DCM for the formation and precipitation of IC complexes, then we see clearly that the diffusive growth, spread and eventual merging of the high DCM concentration zones around each point source with time is analogous to our experimental observation of network formation. This also leads to an important conclusion – that the characteristic time for network formation is basically the characteristic diffusion time between any pair of droplets in the network. Secondly, packing density, which is accounted for in our model by the spacing between point sources, dramatically impacts the network formation process. The closer the point sources are, the more rapid is the growth of high concentration zones around each point source, thus implying a more rapid formation of the IC network. In the actual experimental

situation, loosely packed drops might not lead to the formation of a network at all (Figure 2f), since the DCM also leaves the medium surrounding the droplets and into the atmosphere. Thus, we are led to the counterintuitive conclusion that the more closely packed the droplets are, the faster and more likely is the formation of a connected network of IC crystalline aggregates surrounding the droplet ensemble, and thus the greater the system stability. To conclude this brief analysis, we note here that the simple *free* diffusion model above, while explaining (and unifying) all our observations, does not account for *hindered* outward diffusion of DCM through a growing shell of solid ICs, which could also lead to self-terminating shell growth around droplets, especially at low packing densities.

Next, we demonstrate an application of these transient colloidal crystalline networks in enabling advanced materials synthesis, specifically in microfluidic emulsion-based crystallization, which has been recently used to fabricate 'designer' pharmaceutical microparticles comprising mixtures of drugs and excipients with tailored structure, composition and crystallinity.[22,23,28,29] In our demonstration, monodisperse O/W emulsions (~50 μL), with ROY (a well-studied model pharmaceutical drug molecule[30]) in DCM (250 mg/mL) as dispersed phase and 1.5 wt% PVA aqueous solution as continuous phase, were dispensed into a glass petri dish maintained at 25 ^{o}C on a hot plate with a pre-dispensed 2 mm-thick film of 1 wt% β-cyclodextrin aqueous solution. The following sequence of phenomena was observed (Figure 3a-d): (i) instant turbidity around the droplets (as also described above) due to precipitation of ICs, (ii) DCM evaporation and droplet shrinkage (t ~ 0 - 60 min) to ~60% of the dispensed diameter, coupled with simultaneous formation of a three-dimensional colloidal network encasing and isolating individual droplets, and (iii) onset of crystal nucleation with a concomitant dissolution of the crystal network. Droplet shrinkage occurred at a linear rate of ~0.019 μm/s, as measured from time-lapse microscopy, and was nearly arrested at ~60 min, beyond which no further change of droplet diameter could be measured (see Figure S3 and accompanying discussion in the Supporting Information). Furthermore, and interestingly, this measured shrinkage rate was lower than

that measured for the case of ROY-DCM droplets of the same composition in the absence of β-cyclodextrin (~0.026 μm/s), possibly due to two reasons - hindered outward diffusion of the DCM through the shell of ICs, and local 'hotspots' in DCM concentration around the droplets, which decrease the gradient for outward diffusion, as highlighted in the simple model above. The first crystal nucleation event was observed at t ~ 60 min, while the dissolution of the network was nearly complete at t ~ 90 min. During the crystallization process, droplets were observed to be stable with minimal movement, unlike other typical cases of evaporative crystallization, where evaporation-driven coalescence[29] and secondary nucleation are persistent challenges.[31] Furthermore, since droplet solidification occurred by a nucleation and growth-based crystallization mechanism, each droplet retained it's spherical shape until a nucleation event occurred within the interior. Monodisperse crystalline spherical microparticles of ROY with a diameter ~100 μm were obtained (with a standard deviation of ~2%), as shown in Figure 3e-f. DSC characterization revealed the polymorphic composition to be dominated by the Y form of ROY.[30] (See Supporting Information Figure S5 – DSC plot). It is worth noting here that crystallization across the entire droplet ensemble took nearly 150 min; hence a part of the process occurred in the absence of the colloidal network. While this was not a limitation in this simple demonstration, we note that the relative rates of both colloidal network formation/dissolution and that of crystallization can be easily controlled, for example, by tuning the film thickness of pre-dispensed β-cyclodextrin solution, the concentrations of ROY or the β-cyclodextrin aqueous solution, or even the DCM partial pressure in the headspace above the β-cyclodextrin film.

To highlight the remarkable degree of control over crystallization enabled by the above approach, we present results from the case when the droplets were dispensed in a film of ultrapure water instead of β-cyclodextrin solution, in which case no extended network stabilizing the droplets was formed. In this case, droplet movement due to evaporation-driven convection caused severe secondary nucleation,

which involved contact between crystallized particles and supersaturated droplets leading to the formation of large crystal agglomerates with uncontrolled shapes and sizes (Supporting Information Figure S4 and Video). In the extreme case where the entire petri dish was covered by a closely-packed monolayer of droplets to preclude drop motion, severe secondary nucleation resulted in an extremely low yield of the desired spherical microparticles (Figure 4a). On the contrary, in the case where droplets were collected in a film of β-cyclodextrin solution, consistent with our inference from the diffusion model for the network formation process, more closely packed droplets resulted in rapid formation of the network and highly monodisperse particles were obtained (Figure 4b).

In summary, we have demonstrated the dynamic assembly of a transient, colloidal crystal network, which forms precisely at the interface of each emulsion droplet instantaneously via outward diffusion of a guest molecule from the droplets, and then further develops into a three-dimensional network of ICs for complete isolation of individual droplets in the ensemble. This diffusion-driven colloidal network thus offers both instant and long-term stability of the emulsion system, holding each droplet in its place. As the guest molecule is depleted from the system, these aggregates dissolve back into the aqueous solution. The colloidal crystal network produced has much to offer in areas where emulsion stability and isolation of the emulsion droplets are essential. We demonstrate the feasibility and utility of the method with a case of microfluidic emulsion-based crystallization, where monodisperse spherical crystalline microparticles of a model drug are obtained with exquisite control. A general extension of these concepts to any emulsion-based system requires that the dispersed phase contain a guest molecule capable of forming insoluble inclusion complexes with β-cyclodextrin – a fairly flexible criterion given the large number of molecules that have been demonstrated to do so in recent years. Our ongoing work beyond this initial proof-of-concept demonstration involves detailed studies of the dynamics of colloidal crystal network formation/dissolution. Specifically, the effect of film thickness and concentration of β-

cyclodextrin solution on crystal network formation/dissolution are of particular interest, in order to design process parameters that ensure complete isolation in any potential systems of application.

EXPERIMENTAL SECTION

Materials Poly(vinyl) alcohol (PVA) (M.W. - 67,000), β-cyclodextrin (≥ 99% HPLC) and dichloromethane (DCM) (99.5%) were purchased from Sigma-Aldrich (Singapore) and used as received. 5-methyl-2-[(2-nitrophenyl)amino]-3-thiophenecarbonitrile (ROY) was purchased from Dr Macs Bio-Pharma Private Limited, India, and further purified by cooling re-crystallization. Ultrapure water (18.3 MΩ) obtained using a Millipore Milli-Q purification system was used to prepare aqueous PVA and β-cyclodextrin solution. Harvard PHD 22/2000 series syringe pumps were used to dispense fluids into the emulsion generator. Square and cylindrical glass capillaries of ID 1 mm and 0.7 mm respectively were purchased from Arte glass associates Co. Ltd., Japan.

Methods

Emulsion Generation O/W emulsions were generated using a glass capillary microfluidic setup (A schematic of the experimental setup is provided in the supporting information Figure S1). The axisymmetric coaxial glass capillary flow-focusing device was assembled using a square and round capillary, as demonstrated by our group previously.[22,28] The surface of the round capillary was hydrophilized by treatment with oxygen plasma (100 W) for 120 s. The aqueous continuous phase (W) used was a 1.5 wt% PVA aqueous solution. The dispersed phase (O) was one of the following: (i) DCM, or (ii) ROY in DCM (250 mg/mL). W and O phases were infused from the two ends of the square capillary through the outer coaxial region using syringe pumps (Harvard PHD 22/2000 series) at flow rates of 80 and 40 μL/min respectively. The emulsion droplets were formed by hydrodynamic flow focusing through the nozzle of the inner round capillary.

Evaporation of Emulsions: 5.1 cm ID glass petri dishes were used for sample collection. Approximately 50 μL of O/W emulsions were dispensed directly into each glass petri dish containing a 2 mm film of 1% wt β-cyclodextrin aqueous solution. Evaporation of DCM droplets and evaporative crystallization were performed at 25 ^{o}C, measured with a thermometer (Lutron TM-914C), on a hot plate (set T = 30 ^{o}C) and at ambient humidity (55%). Optical microscopy images were captured using a QImaging MicroPublisher 5.0 RTV camera mounted on an Olympus SZX7 microscope. A Leica CLS 150 XE light source was used. A silicon wafer was placed beneath the glass petri dishes on the hot plate for the purpose of better visualization, as the IC precipitates formed were white in color and the wafer created a black background for the images.

Harvesting DCM-β-cyclodextrin IC crystals: Due to the transient nature of the IC colloidal crystal formation process, it was not feasible to harvest the IC crystals directly from the glass well. As an alternative, we observed the IC crystal aggregate formation process at the interface between DCM and 1 wt% β-cyclodextrin aqueous solution in a GC vial. 600 μL of DCM was transferred into the GC vial first, due to its higher density (1.325 g/mL at 25ºC as specified on safety data sheet of Sigma-Aldrich) than water, followed by careful addition of another 600 μL of 1% wt β-cyclodextrin aqueous solution on top. Immediate turbidity was observed both at the interface and inside the aqueous phase, with the former being starkly more apparent than the latter. The GC vial was then sealed and kept for 7 days to allow more IC crystals to form through diffusion of DCM. A thick, white turbid layer formed at the interface and was harvested for further characterization. (Supporting Information, Figure S2)

Characterization

The size distribution, morphology and polymorphism of the ROY spherical agglomerates obtained were characterized by using microscopic image analysis, field emission scanning electron microscopy (FESEM), and differential scanning calorimetry (DSC). The DCM-β-cyclodextrin IC crystals harvested from the GC vial were characterized by FESEM. A field emission scanning electron microscope (JEOL JSM-6700F) at 5 kV accelerating voltage was used to acquire further structural information on the ROY

SAs and DCM-β-cyclodextrin IC crystals. All samples were prepared using silicon wafer pieces and carbon tape on conventional SEM stubs. Subsequently, samples were coated with ~10 nm of platinum by sputter coating. The DSC thermograms were obtained using a Mettler Toledo DSC 882 apparatus. Around 5 mg of sample was crimped in a sealed aluminum pan and heated at 3 °C/ min from 70°C to 130 °C using an empty sealed pan as a reference.

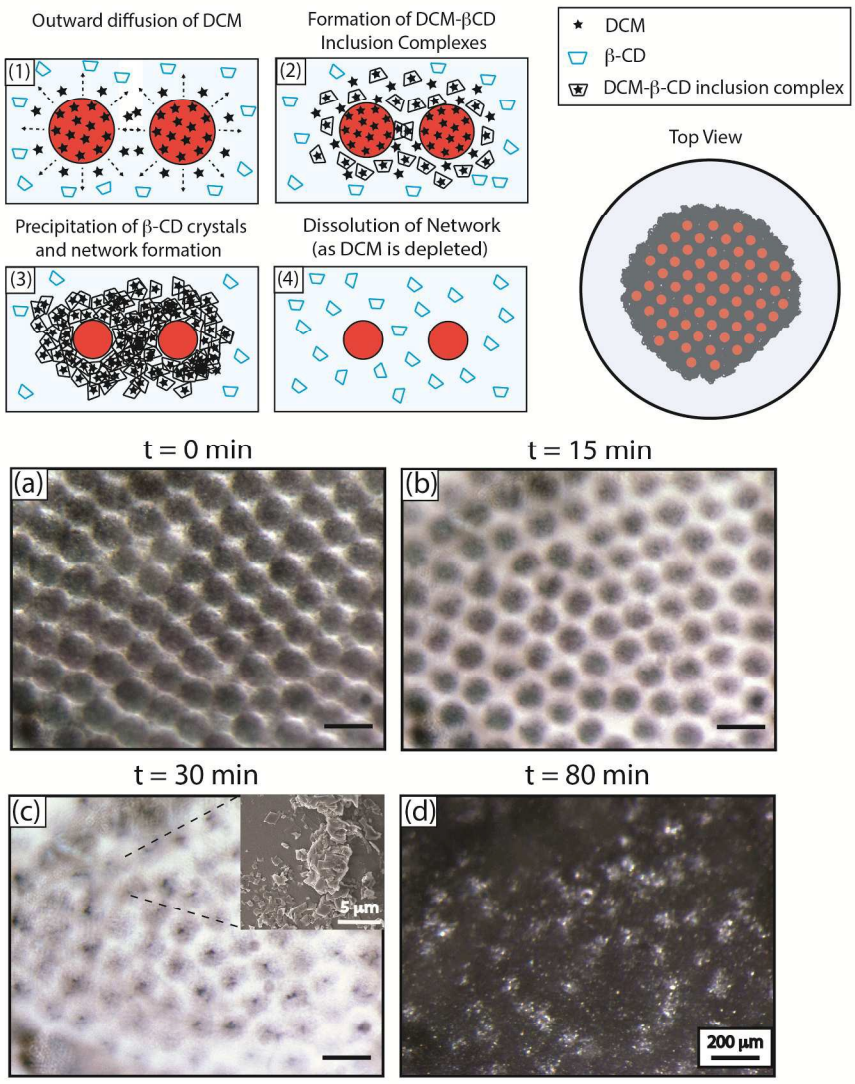

Figure 1. A phenomenological schematic of our method - microfluidic 'oil' droplets dispersed in an aqueous continuous phase, and containing a guest molecule (in our case, a volatile molecule – dichloromethane (DCM)) that can form inclusion complexes with β-cyclodextrin, are collected and incubated in a static thin film containing an aqueous β-cyclodextrin solution. The schematic is a top-view of the incubated ensemble, and depicts the various stages in the network formation process. (a)-(d) Time-lapse stereomicroscopic images of an ensemble of microfluidic DCM droplets (dispersed in water, and generated from a capillary device) incubated in a thin (~2 mm) film of aqueous 1% wt β-cyclodextrin solution under ambient conditions. The images capture the various stages in the colloidal

network formation process, including solvent diffusion (droplet shrinkage), formation and precipitation of ICs, formation of IC crystal network, and dissolution of aggregates upon depletion of DCM from the solution. The inset in 1(c) shows an FESEM image of harvested IC crystals (see main text for details)

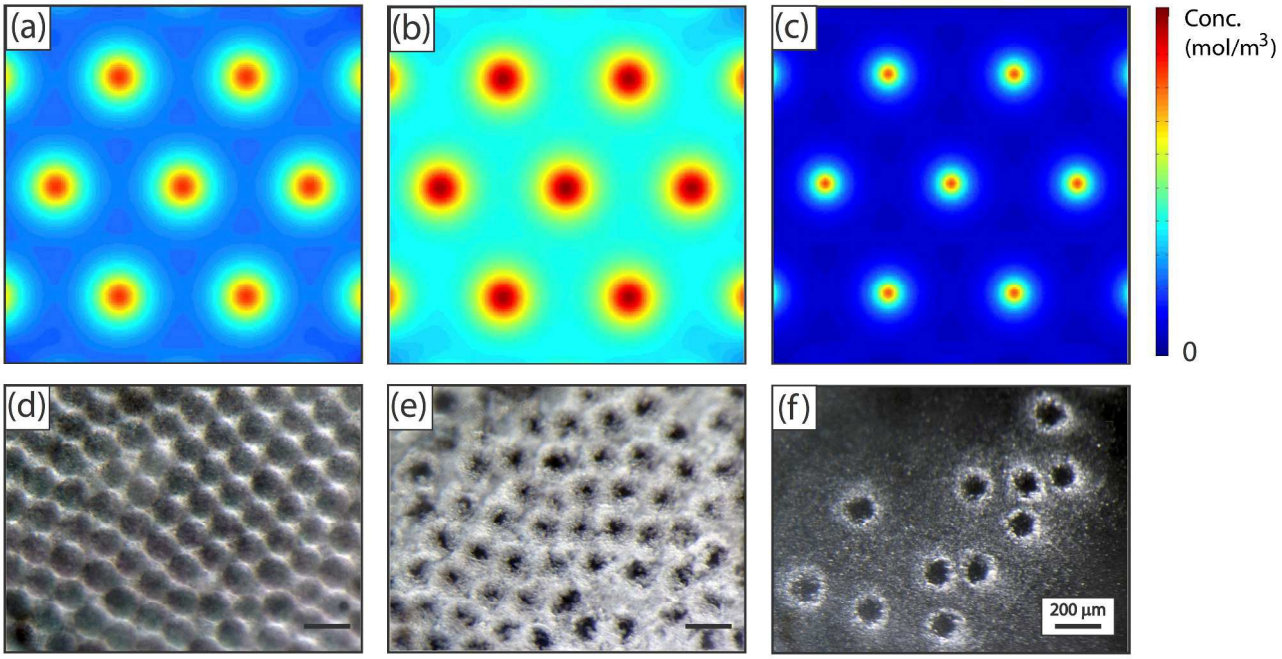

Figure 2. (a)-(c) Snapshots of concentration maps from the analytical solution for diffusion from a 2-D hexagonally-ordered array of point sources releasing DCM (details in supporting information) at a time-dependent rate. 2(a) and (b) are results for the same spacing between point sources (equivalent to one droplet diameter in our experiments), and at 5 and 10 time units respectively, while (c) is a result for a doubled spacing between point sources, and at 10 time units. These plots in the first row of the figure serve as useful visual analogues for the observed network formation behavior; the corresponding experimental image sequence is provided in the second row. Stereomicroscope images of a close-packed droplet ensemble, captured immediately after dispensing the droplets ($t \sim 0$) (2(d)), and at $t \sim 30$ min (2(e)), show the evolution of the network in time, and the stereomicroscope image of a loosely packed droplet ensemble, captured at $t \sim 30$ min (2(f)) shows the effect of large droplet spacing, in which network formation is not observed.

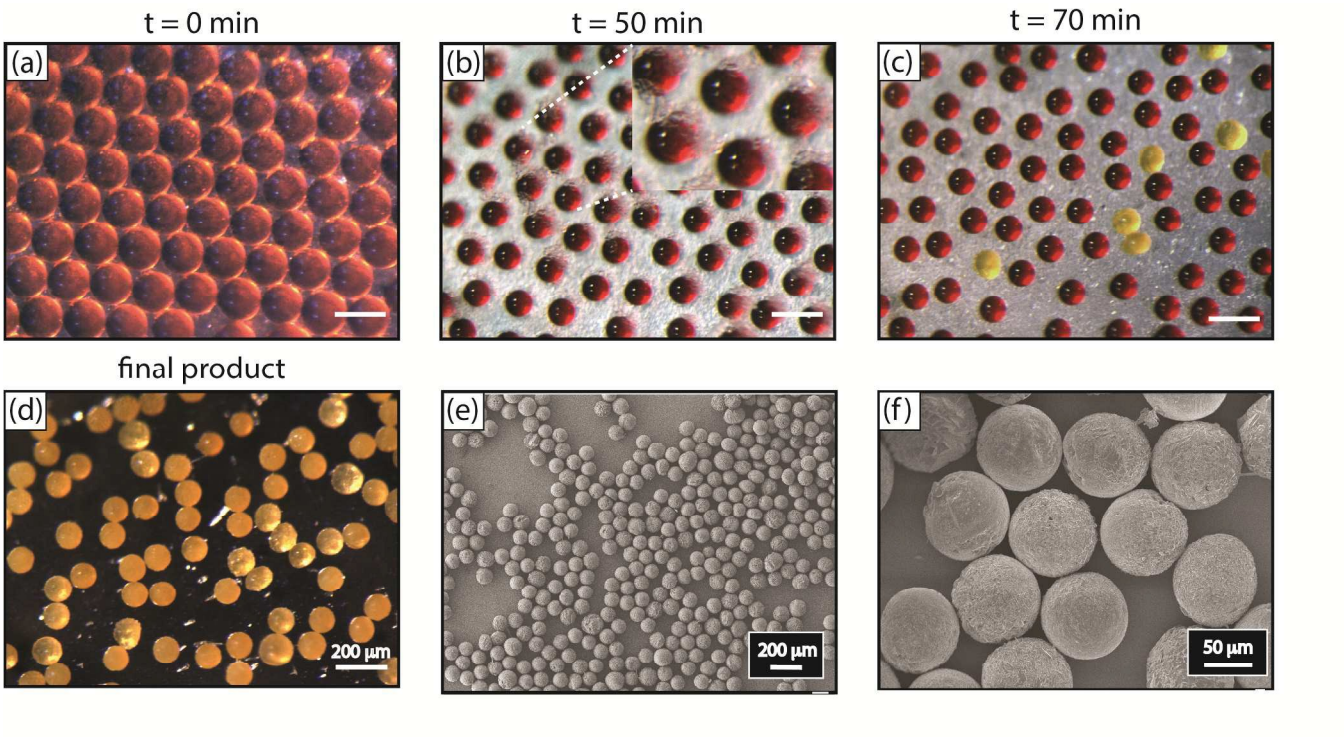

Figure 3. Time series of stereomicroscopic images of (a) ROY-containing microfluidic emulsion droplets dispensed in an aqueous 1% wt β-cyclodextrin solution, (b) colloidal IC network formation along with droplet shrinkage, (c) nucleation of ROY within the droplets and dissolution of the network, and (d) final crystalline microgranules of ROY after complete network dissolution. Scale bars represent 200 μm unless specified otherwise. (e) – (f) FESEM images of spherical ROY microgranules obtained via this method, highlighting the monodispersity and smooth surface morphology (For further characterization of crystallinity, please refer to the supporting information).

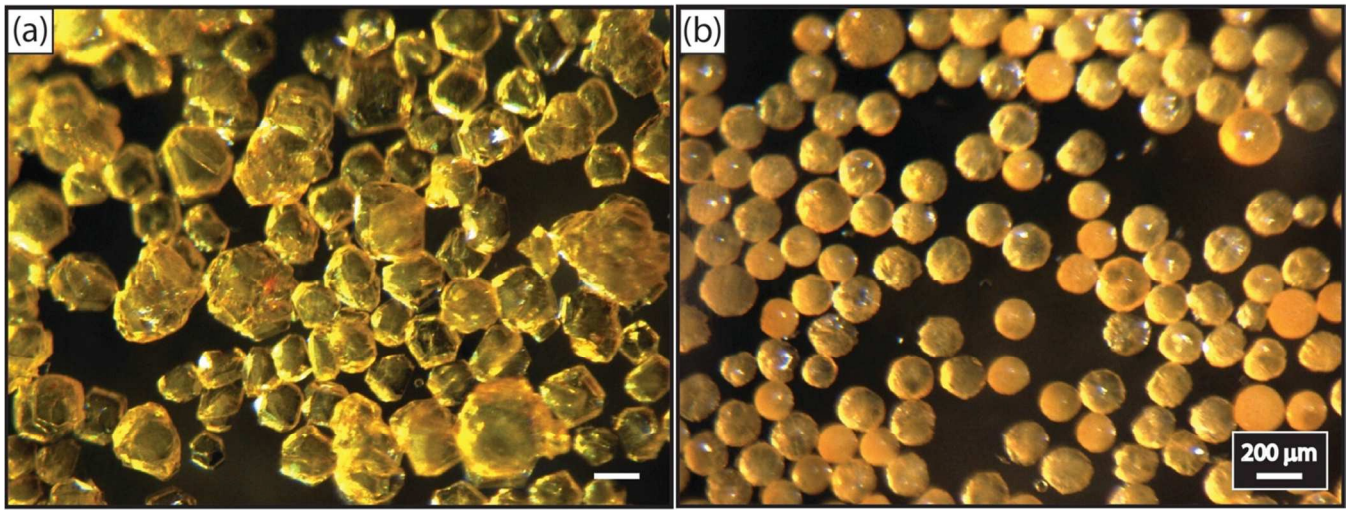

Figure 4. Comparison of spherical, crystalline ROY microgranules obtained from (initially) close-packed microfluidic droplet ensembles in: (a) ultrapure water and (b) 1% β-cyclodextrin solution (imaged *after* dissolution of the β-cyclodextrin network). As is evident, extensive agglomeration was observed in the first case, mainly due to cascaded secondary nucleation events occurring on direct droplet contact. In sharp contrast, the second case exhibited a uniform population of spherical crystalline particles with no agglomeration or shape distortion, highlighting the impact of our transient network stabilization strategy.

References

1 J. T. Wang, J. Wang and J. J. Han, *Small*, 2011, **7**, 1728−1754.

2 M.T. Guo, A. Rotem, J. A. Heyman and D. A. Weitz, *Lab Chip*, 2012, **12**, 2146-2155.

3 R. Seemann, M. Brinkmann, T. Pfohl and S. Herminghaus, *Rep. Prog. Phys.*, 2012, **75**, 016601.

4 J-C. Baret, *Lab Chip*, 2012, **12,** 422-433.

5 C. N. Baroud, F. Gallaire and R. Dangla, *Lab Chip*, 2010, **10**, 2032-2045.

6 S. Arditty, V. Schmitt, J. Giermanska-Kahn, and F. Leal-Calderon, *J Colloid Interface Sci,* 2004, **275**, 659-664.

7 T. Sakai, *Curr. Opin. Colloid Interface Sci*, 2008, **13**, 228-235.

8 Q. Yuan, O. J. Cayre, M. Manga, R. A. Williams, and S. Biggs, *Soft Matter,* 2010, **6**, 1580.

9 P. N. Sturzenegger, U. T. Gonzenbach, S. Koltzenburg, and L. J. Gauckler, *Soft Matter,* 2012, **8**, 7471.

10 B. G. Mathapa and V. N. Paunov, *J. Mater. Chem. A,* 2013, **1**, 10836.

11 B. G. Mathapa and V. N. Paunov, *Phys Chem Chem Phys,* 2013, **15**, 17903-17914.

12 R. Aveyard, B. P. Binks, and J. H. Clint, *Adv. Colloid Interface Sci,* 2003, **100-102**, 503-546.

13 S. Ghosh, T. Tran, and D. Rousseau, *Langmuir,* 2011, **27**, 6589-6597.

14 B. S. Ghotra, S. D. Dyal, and S. S. Narine, *Food Res Int,* 2002, **35**, 1015-1048.

15 D. Johansson, B. Bergenståhl, and E. Lundgren, *J. Am. Oil Chem. Soc,* 1995, **72**, 939-950.

16 M. Vaisey-Genser and G. Ylimaki, *Cereal foods world.,* 1989, **34***,* 246-258.

17 X. Li, H. Li, Q. Xiao, L. Wang, M. Wang, X. Lu*, et al.*, *Phys Chem Chem Phys,* 2014, **16**, 14059-14069.

18 D. Duchêne, A. Bochot, S.-C. Yu, C. Pépin, and M. Seiller, *Int. J. Pharm,* 2003, **266**, 85-90.

19 K. Shimada, K. Fujikawa, K. Yahara, and T. Nakamura, *J. Agric. Food Chem,* 1992, **40**, 945-948.

20 M. Inoue, K. Hashizaki, H. Taguchi, and Y. Saito, *J. Oleo Sci.,* 2009, **58**, 85-90.

21 M. V. Rekharsky and Y. Inoue, *Chem. Rev,* 1998, **98**, 875-1918.

22 A. I. Toldy, A. Z. M. Badruddoza, L. Zheng, T. A. Hatton, R. Gunawan, R. Rajagopalan*, et al.*, *Cryst. Growth Des.*, 2012, **12**, 3977-3982.

23 R. A. L. Leon, W. Y. Wan, A. Z. M. Badruddoza, T. A. Hatton, and S. A. Khan, *Cryst. Growth Des.,* 2014, **14**, 140-146.

24 A. W. Lantz, S. M. Wetterer, and D. W. Armstrong, *Anal Bioanal Chem,* 2005, **383**, 160-166.

25 A. Bochot, L. Trichard, G. L. Bas, H. Alphandary, J. L. Grossiord, D. Duchêne*, et al.*, *Int. J. Pharm,* 2007, **339**, 121-129.

26 I. Sanemasa, J.-S. Wu, and K. Toda, *Bull. Chem. Soc. Jpn,* 1997, **70**, 365-369.

27 W. M. Deen, *Analysis of Transport Phenomena.* New York: Oxford University Press, 1998.

28 R. A. L. Leon, A. Z. M. Badruddoza, L. Zheng, E. W. Q. Yeap, A. I. Toldy, K. Y. Wong*, et al.*, *Cryst. Growth Des.*, 2015, **15**, 212-218.

29 H. B. Eral, M. O'Mahony, R. Shaw, B. L. Trout, A. S. Myerson, and P. S. Doyle, *Chem. Mater,* 2014, **26**, 6213-6220.

30 L. Yu, *Acc. Chem. Res.*, 2010, **43**, 1257-1266.

31 A. I. Toldy, L. Zheng, A. Z. M. Badruddoza, T. A. Hatton, and S. A. Khan, *Cryst. Growth Des.*, 2014, **14**, 3485-3492.